

Predicting potential drug targets and repurposable drugs for COVID-19 via a deep generative model for graphs

Sumanta Ray^{1*,+}, Snehalika Lall²⁺, Anirban Mukhopadhyay³, Sanghamitra Bandyopadhyay², and Alexander Schönhuth^{1,4*}

¹Centrum Wiskunde & Informatica, Science Park 123, 1098 XG Amsterdam, The Netherlands

²Machine Intelligence Unit, Indian Statistical Institute, Kolkata, India.

³Department of Computer Science and Engineering, University of Kalyani, Kalyani, India

⁴Genome Data Science, Bielefeld University, Bielefeld, Germany

*Sumanta.Ray@cwil.nl

+these authors contributed equally to this work

ABSTRACT

Coronavirus Disease 2019 (COVID-19) has been creating a worldwide pandemic situation. Repurposing drugs, already shown to be free of harmful side effects, for the treatment of COVID-19 patients is an important option in launching novel therapeutic strategies. Therefore, reliable molecule interaction data are a crucial basis, where drug-/protein-protein interaction networks establish invaluable, year-long carefully curated data resources. However, these resources have not yet been systematically exploited using high-performance artificial intelligence approaches. Here, we combine three networks, two of which are year-long curated, and one of which, on SARS-CoV-2-human host-virus protein interactions, was published only most recently (30th of April 2020), raising a novel network that puts drugs, human and virus proteins into mutual context. We apply Variational Graph AutoEncoders (VGAEs), representing most advanced deep learning based methodology for the analysis of data that are subject to network constraints. Reliable simulations confirm that we operate at utmost accuracy in terms of predicting missing links. We then predict hitherto unknown links between drugs and human proteins against which virus proteins preferably bind. The corresponding therapeutic agents present splendid starting points for exploring novel host-directed therapy (HDT) options.

Introduction

The pandemic of COVID-19 (Coronavirus Disease-2019) has affected more than 6 million people. So far, it has caused about 0.4 million deaths in over 200 countries worldwide (<https://coronavirus.jhu.edu/map.html>), with numbers still increasing rapidly. COVID-19 is an acute respiratory disease caused by a highly virulent and contagious novel coronavirus strain, SARS-CoV-2, which is an enveloped, single-stranded RNA virus¹. Sensing the urgency, researchers have been relentlessly searching for possible therapeutic strategies in the last few weeks, so as to control the rapid spread.

In their quest, drug repurposing establishes one of the most relevant options, where drugs that have been approved (at least preclinically) for fighting other diseases, are screened for their possible alternative use against the disease of interest, which is COVID-19 here. Because they were shown to lack severe side effects before, risks in the immediate application of repurposed drugs are limited. In comparison with de novo drug design, repurposing drugs offers various advantages. Most importantly, the reduced time frame in development suits the urgency of the situation in general. Furthermore, most recent, and most advanced artificial intelligence (AI) approaches have boosted drug repurposing in terms of throughput and accuracy enormously. Finally, it is important to understand that the 3D structures of the majority of viral proteins have remained largely unknown, which raises the puts up the obstacles for direct approaches to work even higher.

The foundation of AI based drug repurposing are molecule interaction data, optimally reflecting how drugs, viral and host proteins get into contact with each other. During the life cycle of a virus, the viral proteins interact with various human proteins in the infected cells. Through these interactions, the virus hijacks the host cell machinery for replication, thereby affecting the normal function of the proteins it interacts with. To develop suitable therapeutic strategies and design antiviral drugs, a comprehensive understanding of the interactions between viral and human proteins is essential².

When watching out for drugs that can be repurposed to fight the virus, one has to realize that targeting single virus proteins easily leads to the viruses escaping the (rather simpleminded) attack by raising resistance-inducing mutations. Therefore, host-

directed therapies (HDT), which target human proteins that represent important carriers for the virus to enter and manipulate the human cells, offer an important supplementary strategy³. Unlike strategies that directly target the proteins of the virus, HDT are thought to be less prone to developing resistance, because human proteins are less affected by mutations, and therefore represent more sustainable drug targets. For establishing HDT, one has to identify proteins that are crucial for maintenance and perseverance of the disease causing virus in the human cells. Once such proteins are targeted, the replication machinery of the virus falls apart.

For all these reasons, repurposing drugs for HDT against COVID-19 has great potential. Moreover, it provides hope for rapid practical implementation because of the lack of side effects.

Because the basis for drug repurposing screens are molecule interaction data, biological interaction networks offer invaluable resources, because they have been carefully curated and steadily refined for many years. This immediately points out that network based repurposing screens offer unprecedented opportunities in revealing targets for HDT's, which explains the recent popularity of such approaches in general⁴. Evidence for the opportunities is further provided by successful approaches based on viral-host networks in particular^{5,6}, having led to therapy options for treating Dengue⁷, HIV⁸, Hepatitis C⁹ and Ebola¹⁰. Beyond fighting viruses, treatments for various other diseases have been developed^{11,12}.

Since the outbreak of COVID-19, a handful of research groups have been trying to exploit network resources, developing network algorithms for the discovery of drugs that can be repurposed to act against SARS-CoV-2. The first attempt was made by Zhou et al.¹³ through an integrative network analysis, followed by Li et al.¹⁴, who combined network data with a comparative analysis on the gene sequences of different viruses to obtain drugs that can potentially be repurposed to act against SARS-CoV-2.

Shortly thereafter, Gordon et al.¹⁵ conducted pioneering work by generating a map that juxtaposes SARS-CoV-2 proteins with human proteins that were found to interact in affinity-purification mass spectrometry (AP-MS) screens. Furthermore, in independent work, Dick et al.¹⁶ identified high confidence interactions between human proteins and SARS-CoV-2 proteins using sequence-based PPI predictors (a.k.a. PIPE4 & SPRINT).

Both of the studies^{15,16} on SARS-CoV-2 provide data that had so far been urgently missing in the fight against COVID-19. Only now, we are able to link existing (long term curated and highly reliable) drug-protein and human protein-protein interaction data with proteins of SARS-CoV-2. In other words, only now we can draw links between the molecular agents of the virus and existing drugs on a scale that is sufficiently large to allow for systematic high throughput repurposing screens. Still, of course, it remains to design, develop and implement the corresponding strategies in order to exploit the now decisively augmented resources.

As above-mentioned, in order to exploit resources to a maximum, one optimally makes use of sufficiently advanced AI techniques. In this work, to the best of our knowledge for the first time, we combine all arguments raised above.

- (1) We link existing high-quality, long-term curated and refined, large scale drug/protein - protein interaction data with
- (2) molecular interaction data on SARS-CoV-2 itself, raised only a handful of weeks ago,
- (3) exploit the resulting overarching network using most advanced, AI boosted techniques
- (4) for repurposing drugs in the fight against SARS-CoV-2
- (5) in the frame of HDT based strategies.

As for (3)-(5), we will highlight interactions between SARS-Cov-2-host protein and human proteins important for the virus to persist using most advanced deep learning techniques that cater to exploiting network data. We are convinced that many of the fairly broad spectrum of drugs we raise will be amenable to developing successful HDT's against COVID-19.

Results

In the following, we will first describe the workflow of our analysis pipeline and the basic ideas that support it.

We proceed by carrying out a simulation study that proves that our pipeline accurately predicts missing links in the encompassing drug - human protein - SARS-CoV-2-protein network that we raise and analyze. Namely we demonstrate that our (high-performance, AI supported) prediction pipeline accurately re-establishes links that had been explicitly removed before. This provides sound evidence that the interactions that we predict in the full network most likely reflect true interactions between molecular interfaces.

Subsequently, we continue with the core experiments. We predict links to be missing in the full (without artificially having removed links), encompassing drug - human protein - SARS-CoV-2-protein network, raised by combining links from year-long curated resources on the one hand and most recently published COVID-19 resources on the other hand. As per our simulation study, a large fraction, if not the vast majority of the predictions establish true, hence actionable interactions between drugs on the one hand and SARS-CoV-2 associated human proteins (hence of use in HDT) on the other hand.

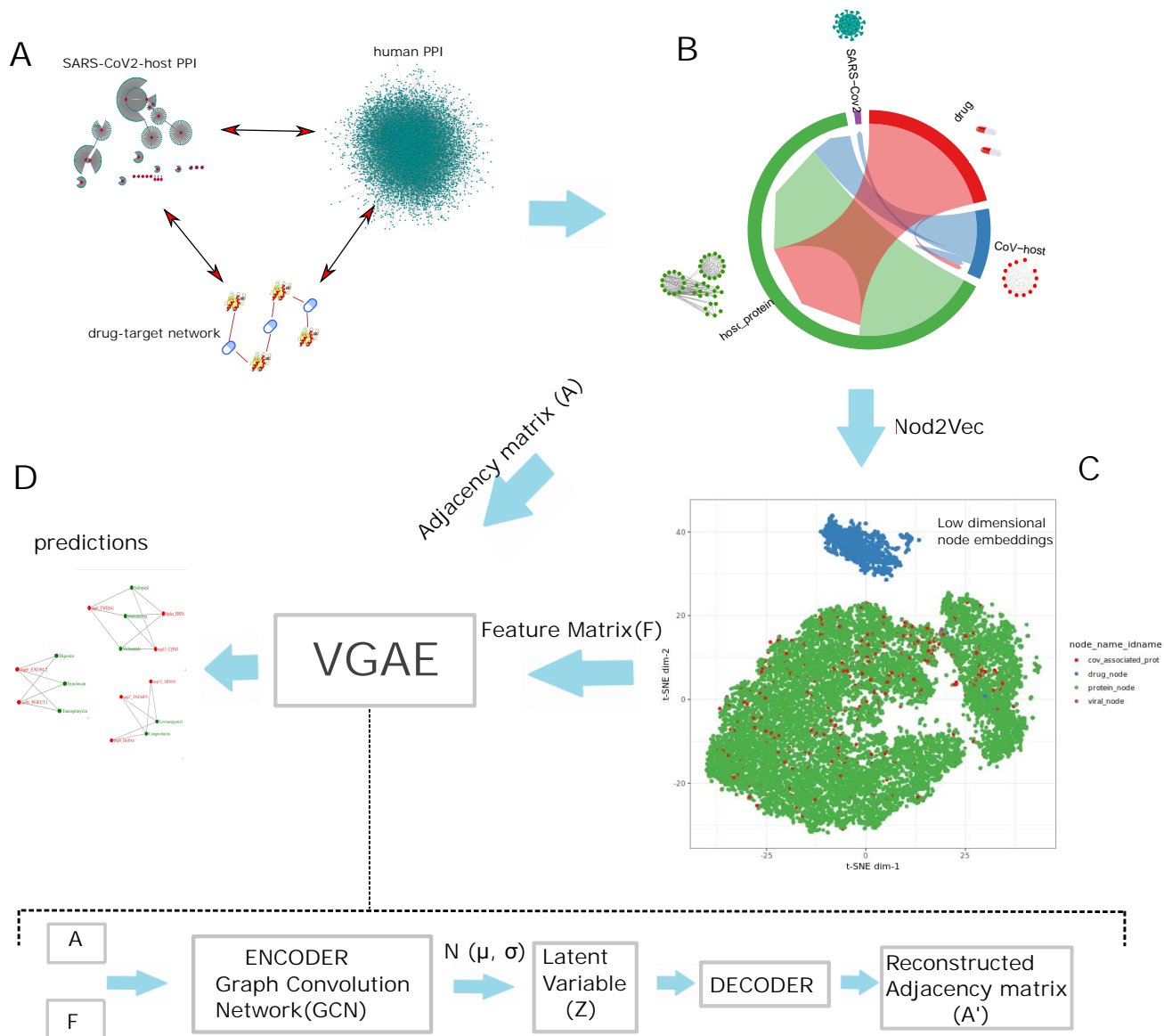


Figure 1. Overall workflow of the proposed method: The three networks SARS-CoV-2-host PPI, human PPI, and drug-target network (Panel-A) are mapped by their common interactors to form an integrated representation (Panel-B). The neighborhood sampling strategy Node2Vec converts the network into fixed-size low dimensional representations that preserve the properties of the nodes belonging to the three major components of the integrated network (Panel-C). The resulting feature matrix (F) from the node embeddings and adjacency matrix (A) from the integrated network are used to train a VGAE model, which is then used for prediction (panel-D).

For the purposes of high-confidence validation, we carry out a literature study on the overall 92 drugs we put forward. For this, we inspect the postulated mechanism-of-action of the drugs in the frame of several diseases, including SARS-CoV and MERS-CoV driven diseases in particular.

Workflow

See Figure 1 for the workflow of our analysis pipeline and the basic ideas that support it. We will describe all important steps in the paragraphs of this subsection.

Raising a Comprehensive Interaction Network. See A & B in Figure 1. We have combined three interaction networks, two of which represent year-long curated and much refined publicly available resources, namely drug-gene interaction and the human interactome, together compiled from eight different, reliable and publicly accessible sources, and one of which the SARS-CoV-2-human protein-protein-interaction (PPI) network was published only a few weeks ago. The integrated network has four types of nodes:

- 1) SARS-CoV-2 proteins,
- 2) SARS-CoV-2-associated host proteins (CoV-host),
- 3) human proteins other than 2)
- 4) and drugs.

This means that we put drugs, human proteins and SARS-CoV-2 proteins into mutual context via the links provided by this network. However, because the encompassing network is built from three subnetworks, links between nodes from different individual subnetworks are presumably missing. It remains to predict them using an AI approach, preferably of utmost performance. This AI approach needs to identify links across the individual subnetworks. Because new cross-subnetwork links may imply links within the established networks as a consequence, the AI approach should also predict new links within the individual parts of our network, if this is called for.

AI Model First Stage: Node2Vec See C in Figure 1. To bring the link prediction machinery into effect, we raise a model that operates in two stages. First, we employ a network embedding strategy (here: Node2Vec¹⁷), which extracts node features from the integrated network. In a bit more formal detail, Node2Vec converts the adjacency matrix that represents the network into a fixed-size, low-dimensional latent space the elements of which are the feature vectors of the nodes. Thereby, Node2Vec aims at preserving the properties of the nodes relative to their surroundings in the network. For efficiency reasons, Node2Vec makes use of a sampling strategy. The result of this step is a feature matrix (F) where rows refer to nodes and columns refer to the inferred network features.

AI Model Second Stage: Variational Graph Autoencoders (VGAE). See B, C & D in Figure 1. In the next step, we employ variational graph autoencoders (VGAE), as a most recent, graph neural network based technique shown to be of utmost accuracy, to predict links in networks that although missing, are highly likely to exist¹⁸. VGAE's require the original graph, provided by its adjacency matrix A and, optionally, a feature matrix that annotates the nodes of the network with helpful additional information. Often, F does not necessarily refer to the topology of the network itself. Here, however, we do make use of the feature matrix F that was inferred from A itself in the first step. We found that, despite just being an alternative representation of A , using F aided in raising prediction accuracy substantially. This may not be surprising, however, because F consists of knowledge obtained using Node2Vec, which, as being complementary to VGAE's from a methodical point of view, cannot necessarily be revealed by VGAE's itself.

Predicting Missing Links. See D in Figure 1. After training the VGAE, we finally predict links in the encompassing drug-human-virus interaction network that had remained to be missing. For this, we make use of the decoding part of the VGAE, which re-raises the network based on the latent representation the network provided by the encoder. Re-raising the network results in edges between nodes that although not having been explicit before, are imperative to exist relative to the encoded version of the network. Thereby, one predicts links between drugs and SARS-CoV-2-associated human proteins in particular. Although these links had not been explicit elements of the drug-human interaction subnetwork before, their existence is implied by the topological constraints the comprehensive network imposes. Thus, our model predicts both drugs and proteins: repurposing these drugs leads to them targeting the matching proteins. See Figure 1 for the total workflow we just described.

Addressing Computation Time. To reduce the computation time, we used a fast version of VGAE's as proposed by Salha et al.,¹⁹. This fast version relies on a strategy by which to sample nodes. Using several non-overlapping test sets for different numbers of sampling nodes, we evaluated the model based on sampling 5000 nodes as most suitable for our prediction task.

Validation of the Learned Model

Let $G = (V, E)$ be the entire drug-human-virus interaction network in the following, where nodes V represent drugs or proteins and edges E represent interactions between them. We run Node2Vec¹⁷ on G to obtain a feature matrix F where rows can be identified with elements from V and columns represent features extracted from G .

After having computed F , we encode the network G into the embedding space using variational graph autoencoder (VGAE) techniques. In detail, we use the FastGAE model¹⁹ as a version that decisively speeds up the learning process in the decoding phase as a major argument. For encoding, FastGAE utilizes a (popular) Graph Convolutional Network (GCN) encoder. This leads to encoding all nodes into the latent variable based embedding space. Therefore, FastGAE makes use of the original graph adjacency matrix A , which codes the original topology of the graph, and F . Using FastGAE is explained by the fact that in the decoding phase, a new version of the adjacency matrix has to be established, where A is huge ($N \times N$, where N is the number of all drugs, human proteins and SARS-CoV-2 proteins together), which slows down less rapid implementations of VGAE's decisively. To sort out this issue, FastGAE randomly samples subgraphs G_S , referring to smaller sets of nodes $S \subset V$ of size N_S , and reconstructs the corresponding submatrices A_S in several iterations, each of which refers to a different S . Finally, the submatrices of all samples are combined into an overarching matrix \hat{A} , as an approximation of the matrix that gets reconstructed as a whole in the decoding phase of slow approaches. Note that the approximation was shown to be highly accurate¹⁹.

This reduces the training time compared to the general graph autoencoder model. We tested the model performance for a different number of sampled nodes, keeping track of the area under the ROC curve (AUC), average precision (AP) score, and model training time in the frame of a train-validation-test split at proportions 8:1:1. Table 1 shows the performance of the model for sampled sugraph sizes $N_s = 7000, 5000, 3000, 2500$ and 1000. For 5000 sampled nodes, the model’s performance is sufficiently good enough concerning its training time and validation-AUC and -AP score. The average test ROC-AUC and AP score of the model for $N_s=5000$ are 88.53 ± 0.03 and 84.44 ± 0.04 .

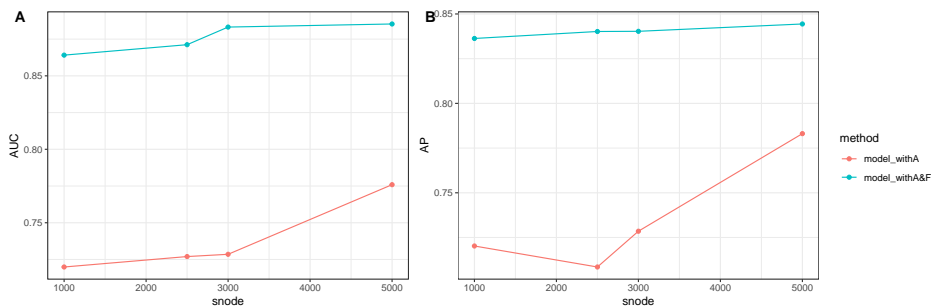
To know the efficacy of the model in discovering the existing edges between only CoV-host and drug nodes, we train the model (with $N_s=5000$) on an incomplete version of the graph where the links between CoV-host and drugs have been removed. We further compute the feature matrix F based on the incomplete graph, and use it. The test set consists of all the previously removed edges. The model performance is no doubt better for discovering those edges between CoV-host and drug nodes (ROC-AUC: 93.56 ± 0.01 AP: 90.88 ± 0.02 for 100 runs).

The FastGAE model is learned with the feature matrix (F) and adjacency matrix (A). The node feature matrix (F) is obtained from A using the Node2Vec neighborhood sampling strategy. The model performance is evaluated with and without using F as feature matrix. Figure 2 shows the average performance of the model on validation sets with and without F as input for the different number of sampling nodes. We calculate average AUC, and AP scores for 50 complete runs of the model. From figure 2, it is evident that including F as feature matrix enhances the model’s performance markedly.

Table 1. Performance of the FastGAE model for different sampling nodes (N_s): mean validation-AUC and -AP scores is computed over last 10 epoch in each run with a train-validation-test split of 8:1:1. Performance is reported over 100 runs for $N_s=7000, 5000, 3000, 2500$ and 1000

N_s	Average Performance on Validation Set		
	AUC (%)	AP (%)	Training Time (in sec)
7000	89.21 ± 0.02	85.32 ± 0.02	1587
5000	89.17 ± 0.03	85.30 ± 0.04	1259
3000	88.91 ± 0.10	85.02 ± 0.04	1026
2500	88.27 ± 0.15	84.88 ± 0.13	998
1000	86.69 ± 0.17	83.58 ± 0.19	816

Figure 2. Performance of the model in validation set with and without using feature matrix (F)



Graph Embedding of the Compiled Network

We use the Node2Vec framework to learn low dimensional embeddings of each node in the compiled network. It uses the Skipgram algorithm of the word2vec model to learn the embeddings, which eventually groups nodes with a similar ‘role’ or having a similar ‘connection pattern’ within the graph. Similar ‘role’ ensures that nodes within the sets/groups are structurally similar/equivalent than the other nodes outside the groups. Two nodes are said to be structurally equivalent if they have identical connection patterns to the rest of the network²⁰. To explore this, we have analyzed the embedding results in two steps. First, we explore structurally equivalent nodes to identify ‘roles’ and similar connection patterns to the rest of the networks, and later use Lovain clustering to examine the same within the groups/clusters. The ‘most_similar’ function of the Node2Vec inspects the structurally equivalent nodes within the network. We find out all the CoV-host nodes which are most similar to the drug nodes. While it is expected to observe nodes of the same types within the neighborhood of a particular node, in some cases, we found some drugs are neighbors of CoV-host proteins with high probability ($pobs > 0.65$). Figure 3 panel-C shows a heatmap of 21 such drugs and their most similar CoV-host proteins. The drugs are hierarchically clustered based on the similarity scores and demonstrated in the row-side dendrogram of the heatmap. A couple of these drugs are frequently used to treat severe allergies, asthma, respiratory diseases, and gastrointestinal infections, which are the main symptoms of COVID patients. Mainly, Dexamethasone, Cetirizine, isoprenaline, Betulinic acid and Clebopride, which are the probable neighbor of CoV-host EXOSC3 (with $pobs$: 0.71, 0.69, 0.67, 0.68 and 0.68, respectively, figure 3, panel-C) have a well-known effect on these diseases. Betulinic acid has antiretroviral, antimalarial, and anti-inflammatory properties and acts as the inhibitors of

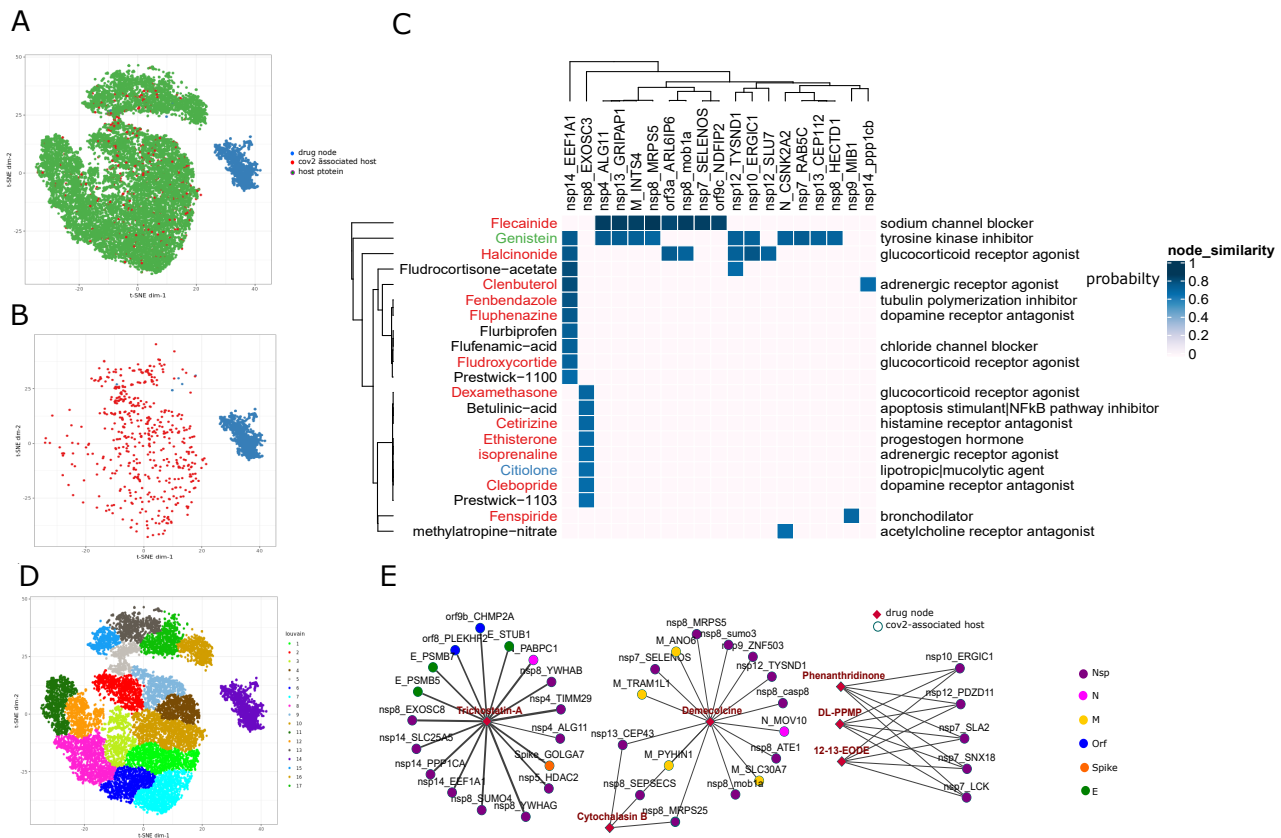


Figure 3. Results of applying Node2Vec on the whole network. Panel-A shows 2-dimensional t-SNE plot of all nodes in the network. Panel-B shows the same for only drug and CoV-host nodes. Panel-C represents heatmap of 21 ‘most similar’ (structurally equivalent or have similar ‘role’) drugs of CoV-hosts. The drugs are colored based on their clinical phase (red–launched, preclinical–blue, phase2/phase3–green and phase-1/ phase-2–black). Panel-D represents visualization of 17 Louvain clusters identified in the low dimensional embedding space. Panel-E shows a network consisting of 6 drugs and their most probable neighbours within the network. These drugs share same Louvain cluster with some CoV-host proteins.

SARS-CoV-2 3CL protease²¹. Some other drugs such as ‘Clenbuterol’ and ‘Fenbendazole’, the probable neighbor of ppp1cb and EEF1A respectively, are used as bronchodilators in asthma.

To explore the closely connected groups, we have constructed a neighborhood graph using the K-th nearest neighbor algorithm from the node embeddings and apply Louvain clustering (Figure 3-panel-C). Although there is a clear separation between host proteins (including CoV-host) cluster and drug cluster, some of the Louvain clusters contain both types of nodes. For example, Louvain cluster-16 and -17 contain four and two drugs along with the other CoV-host proteins, respectively. Figure 3 panel-D represents a network consisting of these six drugs and their most similar CoV-host nodes.

Drug–CoV-host Interaction Prediction

For drug–CoV-host interaction prediction, we exploit Variational Graph Autoencoder (VGAE), an unsupervised graph neural network model, first introduced in¹⁸ to leverage the concept of variational autoencoder in graph-structured data. To make learning faster, we utilized the fastGAE model to take advantage of the fast decoding phase. We have used two data matrices in the fastGAE model for learning: one is the adjacency matrix, which represents the interaction information over all the nodes, and the other one is the feature matrix representing the low-dimensional embeddings of all the nodes in the network. We create a test set of ‘non-edges’ by removing all existing links between drugs and CoV-host proteins from all possible combinations (332 CoV-host × 1302 drugs) of edges. The model is trained on the whole network with the adjacency matrix A and feature matrix F . The trained model is then applied to the test ‘non-edges’ to know the most probable links. We identified a total of 692 most probable links with 92 drugs and 78 CoV-host proteins with a probability threshold of 0.8. The predicted CoV-host proteins are involved in different crucial pathways of viral infection (table 4). The p-values for pathway and GO enrichment are calculated by using the hypergeometric test with 0.05 FDR corrections. Figure 4, Panel-A shows the heatmap of probability scores between predicted drugs and CoV-host proteins. To get more details of the predicted bipartite graph, we

use a weighted bipartite clustering algorithm proposed by J. Beckett²³. This results in 4 bipartite modules (Panel-A figure 4): B1 (11 drugs, 28 CoV-host), B2 (4 drugs, 41 CoV-host), B3 (71 drugs and 4 CoV-host), and B4 (6 drugs and 5 CoV-host). The other panels of the figure show the network diagram of four bipartite modules. B1 contains 11 drugs, including some antibiotics (Anisomycin, Midecamycin), and anti-cancer drugs (Doxorubicin, Camptothecin). B3 also has some antibiotics such as Puromycin, Demeclocycline, Dirithromycin, Geldanamycin, and Chlortetracycline, among them, the first three are widely used for bronchitis, pneumonia, and respiratory tract infections²⁴. Some other drugs such as Lobeline and Ambroxol included in the B3 module have a variety of therapeutic uses, including respiratory disorders and bronchitis. The high confidence predicted interactions (with threshold 0.9) is shown in Figure 5 panel-A. To highlight some repurposable drug combination and their predicted CoV-host target, we perform a weighted clustering (clusterONE)²⁵ on this network and found some quasi-bicliques (shown in Panel-B-E)

We matched our predicted drugs with the drug list recently published by Zhou et al.¹³ and found six common drugs: Mesalazine, Vinblastine, Menadione, Medrysone, Fulvestrant, and Apigenin. Among them, Apigenin has a known effect in the antiviral activity together with quercetin, rutin, and other flavonoids²⁶. Mesalazine is also proven to be extremely effective in the treatment of other viral diseases like influenza A/H5N1 virus.²⁷

Repurposable drugs for SARS-CoV-2

Baclofen and Fisetin

Baclofen, a benzodiazepine receptor (GABAA-receptor) agonist, has a potential role in antiviral associated treatment²⁸. Anti-inflammatory antedecensin fisetin is also tested for antiviral activity, such as for inhibition of Dengue (DENV) virus infection²⁹. It down-regulates the production of proinflammatory cytokines induced by a DENV infection. Both of the drugs are listed in the high confidence interaction set with the three CoV-hosts: TAPT1 (interacted with SARS-CoV-2 protein: orf9c), SLC30A6 (interacted with SARS-CoV-2 protein: orf9c), and TRIM59 (interacted with SARS-CoV-2 protein: orf3a) (Figure 5-panel-C).

Topoisomerase Inhibitors

Topoisomerase Inhibitors play an active role as antiviral agents by inhibiting the viral DNA replication^{30,31}. Some Topoisomerase Inhibitors such as Camptothecin, Daunorubicin, Doxorubicin, Irinotecan and Mitoxantrone are predicted to interact with several CoV-host proteins. It has been demonstrated that the anticancer drug camptothecin (CPT) and its derivative Irinotecan have a potential role in antiviral activity^{32,33}. It inhibits host cell enzyme topoisomerase-I which is required for the initiation as well as completion of viral functions in host cell³⁴. Daunorubicin (DNR) has also been demonstrated as an inhibitor of HIV-1 virus replication in human host cells³⁵. The conventional anticancer antibiotic Doxorubicin was identified as a selective inhibitor of *in vitro* Dengue and Yellow Fever virus replication³⁶. It is also reported that doxorubicin coupling with monoclonal antibody can create an immunoconjugate that can eliminate HIV-1 infection in mice cell³⁷. Mitoxantrone shows antiviral activity against the human herpes simplex virus (HSV1) by reducing the transcription of viral genes in many human cells that are essential for DNA synthesis³⁸.

Histone Deacetylases Inhibitors (HDACi)

Histone Deacetylases Inhibitors (HDACi) are generally used as latency-reversing agents for purging HIV-1 from the latent reservoir like CD4 memory cell³⁹. Our predicted drug list (Table 3) contains two HDACi: Scriptaid and Vorinostat. Vorinostat can be used to achieve latency reversal in the HIV-1 virus safely and repeatedly⁴⁰. Asymptomatic patients infected with SARS-CoV-2 are of significant concern as they are more vulnerable to infect large number of people than symptomatic patients. Moreover, in most cases (99 percentile), patients develop symptoms after an average of 5-14 days, which is longer than the incubation period of SARS, MERS, or other viruses⁴¹. To this end, HDACi may serve as good candidates for recognizing and clearing the cells in which SARS-CoV-2 latency has been reversed.

HSP inhibitor

Heat shock protein 90 (HSP) is described as a crucial host factor in the life cycle of several viruses that includes an entry in the cell, nuclear import, transcription, and replication^{42,43}. HSP90 is also shown to be an essential factor for SARS-CoV-2 envelop (E) protein⁴⁴. In⁴⁵, HSP90 is described as a promising target for antiviral drugs. The list of predicted drugs contains three HSP inhibitors: Tanespimycin, Geldanamycin, and its derivative Alvespimycin. The first two have a substantial effect in inhibiting the replication of Herpes Simplex Virus and Human enterovirus 71 (EV71), respectively. Recently in⁴⁶, Geldanamycin and its derivatives are proposed to be an effective drug in the treatment of COVID-19.

Antimalarial agent/DNA inhibitor, DNA methyltransferase inhibitor, DNA synthesis inhibitor

Inhibiting DNA synthesis during viral replication is one of the critical steps in disrupting the viral infection. The list of predicted drugs contains six such small molecules/drugs, viz., Niclosamide, Azacitidine, Anisomycin, Novobiocin, Primaquine, Menadione, and Metronidazole. DNA synthesis inhibitor Niclosamide has a great potential to treat a variety of viral infections, including SARS-CoV, MERS-CoV, and HCV virus⁴⁷ and has recently been described as a potential candidate to fight the

Table 2. Dataset Description

Index	Dataset Category	Dataset	#Edges	#Nodes	
1	Human PPI	CCSB ⁵⁵	13944	4303	
		HPRD ⁵⁶	39240	9617	
2	SARS-CoV-2-Host PPI	Gordon et al ¹⁵	332	27 (#SARS-CoV-2)	332 (#Host)
		Dick et al ¹⁶	261	6 (#SARS-CoV-2)	202 (#Host)
3	Drug-target interaction	DrugBank (v4.3) ⁵⁷ , ChEMBL ⁵⁸ , Therapeutic Target Database (TTD) ⁵⁹ , PharmGKB database	1788407	1307 (# Drug)	12134 (# Host-target)

SARS-CoV-2 virus⁴⁷. Novobiocin, an aminocoumarin antibiotic, is also used in the treatment of Zika virus (ZIKV) infections due to its protease inhibitory activity. In 2005, Chloroquine (CQ) had been demonstrated as an effective drug against the spread of severe acute respiratory syndrome (SARS) coronavirus (SARS-CoV). Recently Hydroxychloroquine (HCQ) sulfate, a derivative of CQ, has been evaluated to efficiently inhibit SARS-CoV-2 infection *in vitro*⁴⁸. Therefore, another anti-malarial aminoquinolin drug Primaquine may also contribute to the attenuation of the inflammatory response of COVID-19 patients. Primaquine is also established to be effective in the treatment of Pneumocystis pneumonia (PCP)⁴⁹.

Cardiac Glycosides ATPase Inhibitor

Cardiac glycosides have been shown to play a crucial role in antiviral drugs. These drugs target cell host proteins, which help reduce the resistance to antiviral treatments. The antiviral effects of cardiac glycosides have been described by inhibiting the pump function of Na, K-ATPase. This makes them essential drugs against human viral infections. The predicted list of drugs contains three cardiac glycosides ATPase inhibitors: Digoxin, Digitoxigenin, and Ouabain. These drugs have been reported to be effective against different viruses such as herpes simplex, influenza, chikungunya, coronavirus, and respiratory syncytial virus⁵⁰.

MG132, Resveratrol and Captopril

MG132, proteasomal inhibitor is established to be a strong inhibitor of SARS-CoV replication in early steps of the viral life cycle⁵¹. MG132 inhibits the cysteine protease m-calpain, which results in a pronounced inhibition of SARS-CoV-2 replication in the host cell. In⁵², Resveratrol has been demonstrated to be a significant inhibitor MERS-CoV infection. Resveratrol treatment decreases the expression of nucleocapsid (N) protein of MERS-CoV, which is essential for viral replication. As MG132 and Resveratrol play a vital role in inhibiting the replication of other coronaviruses SARS-CoV and MERS-CoV, so they may be potential candidates for the prevention and treatment of SARS-CoV-2. Another drug Captopril is known as Angiotensin II receptor blockers (ARB), which directly inhibits the production of angiotensin II. In⁵³, Angiotensin-converting enzyme 2 (ACE2) is demonstrated as the binding site for SARS-CoV-2. So Angiotensin II receptor blockers (ARB) may be good candidates to use in the tentative treatment for SARS-CoV-2 infections⁵⁴.

In summary, our proposed method predicts several drug targets and multiple repurposable drugs that have prominent literature evidence of uses as antiviral drugs, especially for two other coronavirus species SARS-CoV and MERS-CoV. Some drugs are also directly associated with the treatment of SARS-CoV-2 identified by recent literature. However, further clinical trials and several preclinical experiments are required to validate the clinical benefits of these potential drugs and drug targets.

Table 3. Table shows 92 predicted repurposable drugs

Sl. No.	pubchem id	Drug	Clinical phase	Uses
1	15281	Alexidine	Preclinical	phosphatidylglycerophosphatase inhibitor
2	17150	Apigenin	Preclinical	casein kinase inhibitor cell proliferation inhibitor
3	18998	Baclofen	Launched	benzodiazepine receptor agonist
4	33216	Clopramide	Launched	sodium/chloride cotransporter inhibitor
5	37446	Digoxin	Launched	ATPase inhibitor
6	107704	Digitoxigenin	Preclinical	ATPase inhibitor
7	117069	Ouabain	Launched	ATPase inhibitor
8	59105	Metformin	Launched	insulin sensitizer
9	71063	Piribedil	Launched	dopamine receptor agonist
10	220964	Pergolide	Withdrawn	dopamine receptor agonist
11	76299	Pyrvinium	Launched	androgen receptor antagonist

Table 3 continued from previous page

12	80626	Sirolimus	Launched	mTOR inhibitor
13	86324	Tanespimycin	Phase 3	HSP inhibitor
14	180858	Geldanamycin	Preclinical	HSP inhibitor
15	245370	Alvespimycin	Phase 2	HSP inhibitor
16	93086	Tretinoin	Launched	retinoid receptor agonist retinoid receptor ligand
17	102361	Anisomycin	Preclinical	DNA synthesis inhibitor
18	103692	Atovaquone	Launched	mitochondrial electron transport inhibitor
19	104090	Azacitidine	Launched	DNA methyltransferase inhibitor
20	104487	Benperidol	Launched	dopamine receptor antagonist
21	121586	Sulpiride	Launched	dopamine receptor antagonist
22	104924	Bisacodyl	Launched	laxative
23	105316	Camptothecin	Phase 3	topoisomerase inhibitor
24	108903	Doxorubicin	Launched	topoisomerase inhibitor
25	114021	Irinotecan	Launched	topoisomerase inhibitor
26	115466	Mitoxantrone	Launched	topoisomerase inhibitor
27	107326	Daunorubicin	Launched	RNA synthesis inhibitor topoisomerase inhibitor
28	108095	Digoxigenin	Preclinical	steroid
29	108477	Diltiazem	Launched	calcium channel blocker
30	109280	Emetine	Phase 2	protein synthesis inhibitor
31	118729	Puromycin	Preclinical	protein synthesis inhibitor
32	178082	Chlortetracycline	Launched	protein synthesis inhibitor
33	182249	Midecamycin	Launched	protein synthesis inhibitor
34	199663	Clindamycin	Launched	protein synthesis inhibitor
35	109651	Estropipate	Launched	estrogen receptor agonist
36	110088	Etamsylate	Launched	haemostatic agent
37	111183	Fursultiamine	Launched	vitamin B
38	114689	Medrysone	Launched	glucocorticoid receptor agonist
39	115901	Nadolol	Launched	adrenergic receptor antagonist
40	116238	Naftopidil	Launched	adrenergic receptor antagonist
41	119913	Sotalol	Launched	adrenergic receptor antagonist
42	215415	Metoprolol	Launched	adrenergic receptor antagonist
43	520283	Doxazosin	Launched	adrenergic receptor antagonist
44	116649	Nocodazole	Preclinical	tubulin polymerization inhibitor
45	220050	Paclitaxel	Launched	tubulin polymerization inhibitor
46	117480	Parthenolide	Phase 1	NFkB pathway inhibitor
47	119578	Scriptaid	Preclinical	HDAC inhibitor
48	124043	Vorinostat	Launched	HDAC inhibitor
49	120719	Sulconazole	Launched	sterol demethylase inhibitor
50	123302	Tracazolate	Phase 2	GABA receptor modulator
51	125857	Novobiocin	Launched	bacterial DNA gyrase inhibitor
52	129195	Azacyclonol	Preclinical	histamine receptor antagonist
53	133584	Galantamine	Launched	acetylcholinesterase inhibitor
54	139192	Niclosamide	Launched	DNA replication inhibitor STAT inhibitor
55	145407	Verteporfin	Launched	photosensitizing agent
56	150553	Alprostadil	Launched	prostanoid receptor agonist
57	159244	Fulvestrant	Launched	estrogen receptor antagonist
58	176723	Cantharidin	Launched	protein phosphatase inhibitor
59	179449	Danazol	Launched	estrogen receptor antagonist progesterone receptor agonist
60	186039	MG-132	Preclinical	proteasome inhibitor
61	191423	Ajmaline	Launched	sodium channel blocker
62	245766	Ambroxol	Launched	sodium channel blocker
63	352301	Cinchocaine	Launched	sodium channel blocker

Table 3 continued from previous page

64	193762	Ampyrone	Preclinical	cyclooxygenase inhibitor
65	203449	Dirithromycin	Launched	bacterial 50S ribosomal subunit inhibitor
66	212182	Levonorgestrel	Launched	estrogen receptor agonist glucocorticoid receptor antagonist progesterone receptor agonist progesterone receptor antagonist
67	214498	Mesalazine	Launched	cyclooxygenase inhibitor lipoxygenase inhibitor prostanoid receptor antagonist
68	217727	Naringin	Preclinical	cytochrome P450 inhibitor
69	223747	Primaquine	Launched	antimalarial agent DNA inhibitor
70	255979	Captopril	Launched	angiotensin converting enzyme inhibitor
71	260887	Chlorzoxazone	Launched	bacterial 30S ribosomal subunit inhibitor
72	268568	Demeclocycline	Launched	bacterial 30S ribosomal subunit inhibitor
73	270479	Dihydroergotamine	Launched	serotonin receptor agonist
74	279244	Fenoprofen	Launched	prostaglandin inhibitor
75	291604	Lobeline	Launched	acetylcholine receptor antagonist
76	293538	Luteolin	Phase 2	glucosidase inhibitor
77	295381	Meclofenoxate	Launched	nootropic agent
78	295680	Menadione	Launched	mitochondrial DNA polymerase inhibitor phosphatase inhibitor
79	321706	Sulfaphenazole	Launched	dihydropteroate synthetase inhibitor
80	333068	Zardaverine	Phase 2	phosphodiesterase inhibitor
81	372869	Metronidazole	Launched	DNA inhibitor
82	416788	Resveratrol	Launched	cytochrome P450 inhibitor SIRT activator
83	423536	Fisetin	Preclinical	Aurora kinase inhibitor
84	441851	Morantel	Launched	acetylcholine receptor agonist
85	451754	Kinetin	Launched	cell division inducer
86	461005	Chrysin	Phase 1	breast cancer resistance protein inhibitor
87	471412	Vinblastine	Launched	microtubule inhibitor tubulin polymerization inhibitor
88	472841	Meticrane	Launched	diuretic
89	483385	Ethosuximide	Launched	succinimide antiepileptic
90	494980	Tetraethylenepentamine	Phase 2/Phase 3	superoxide dismutase inhibitor
91	517908	Ticlopidine	Launched	purinergic receptor antagonist
92	543633	Todralazine	Launched	antihypertensive agent

Discussion

In this work, we have successfully generated a list of high-confidence candidate drugs that can be repurposed to counteract SARS-CoV-2 infections. The novelties have been to integrate most recently published SARS-CoV-2 protein interaction data on the one hand, and to use most recent, most advanced AI (deep learning) based high-performance prediction machinery on the other hand, as the two major points. In experiments, we have validated that our prediction pipeline operates at utmost accuracy, confirming the quality of the predictions we have raised.

The recent publication (April 30, 2020) of two novel SARS-CoV-2-human protein interaction resources^{15,16} has unlocked enormous possibilities in studying virulence and pathogenicity of SARS-CoV-2, and the driving mechanisms behind it. Only now, various experimental and computational approaches in the design of drugs against COVID-19 have become conceivable, and only now such approaches can be exploited truly systematically, at both sufficiently high throughput and accuracy.

Here, to the best of our knowledge, we have done this for the first time. We have integrated the new SARS-CoV-2 protein interaction data with well established, long-term curated human protein and drug interaction data. These data capture hundreds of thousands approved interfaces between encompassing sets of molecules, either reflecting drugs or human proteins. As a result, we have obtained a comprehensive drug-human-virus interaction network that reflects the latest state of the art in terms of our knowledge about how SARS-CoV-2 and interacts with human proteins and repurposable drugs.

Table 4. table describing the Gene Ontology (Biological process) and KEGG pathway for 78 CoV-host proteins

Term (GO/KEGG)	p-value	Genes
Herpes simplex infection	0.002142	TRAF2, PPP1CA, CASP8, HLA-A, HCFC1, HLA-G
Viral carcinogenesis	0.003507	TRAF2, YWHAG, CASP8, HLA-A, VDAC3, HLA-G
Endocytosis	0.006957	AP2A2, HLA-A, HSPA6, SMURF1, RAB10, HLA-G
Epstein-Barr virus infection	0.023579	TRAF2, HLA-A, TNFAIP3, HLA-G
Legionellosis	0.030506	EEF1A1, CASP8, HSPA6
Viral myocarditis	0.033704	CASP8, HLA-A, HLA-G
antigen processing and presentation (GO:0019882)	8.04E-05	HLA-H, HLA-A, MR1, RAB10, HLA-G
antigen processing and presentation of peptide antigen via MHC class I (GO:0002474)	2.60E-04	HLA-H, HLA-A, MR1, HLA-G
negative regulation of extrinsic apoptotic signaling pathway via death domain receptors (GO:1902042)	3.46E-04	TRAF2, HMOX1, CASP8, TNFAIP3
antigen processing and presentation of exogenous peptide antigen via MHC class I, TAP-independent (GO:0002480)	6.05E-04	HLA-H, HLA-A, HLA-G
negative regulation of I-kappaB kinase/NF-kappaB signaling (GO:0043124)	6.14E-04	TRIM59, CASP8, TLE1, TNFAIP3
cellular response to heat (GO:0034605)	0.010384	HMOX1, HSPA6, MYOF
nuclear polyadenylation-dependent tRNA catabolic process (GO:0071038)	0.020673	EXOSC8, EXOSC2
nuclear polyadenylation-dependent rRNA catabolic process (GO:0071035)	0.024756	EXOSC8, EXOSC2
antigen processing and presentation of exogenous peptide antigen via MHC class I, TAP-dependent (GO:0002479)	0.028411	HLA-H, HLA-A, HLA-G
type I interferon signaling pathway (GO:0060337)	0.02925	HLA-H, HLA-A, HLA-G
death-inducing signaling complex assembly (GO:0071550)	0.032873	TRAF2, CASP8
low-density lipoprotein particle clearance (GO:0034383)	0.032873	HMOX1, SCARB1
exonucleolytic trimming to generate mature 3'-end of 5.8S rRNA from tricistronic rRNA transcript (GO:0000467)	0.032873	EXOSC8, EXOSC2
U4 snRNA 3'-end processing (GO:0034475)	0.032873	EXOSC8, EXOSC2
interferon-gamma-mediated signaling pathway (GO:0060333)	0.035392	HLA-H, HLA-A, HLA-G
protein processing (GO:0016485)	0.036307	PCSK1, TYSND1, PCSK6
nuclear-transcribed mRNA catabolic process, exonucleolytic, 3'-5' (GO:0034427)	0.036907	EXOSC8, EXOSC2
regulation of sequestering of zinc ion (GO:0061088)	0.036907	SLC30A6, SLC30A7
regulation of immune response (GO:0050776)	0.038229	PVR, HLA-H, HLA-A, HLA-G

For exploiting the new network—already establishing a new resource in its own right—we have opted for most recent and advanced deep learning based technology. A generic reason for this choice is the surge in advances and the resulting boost in operative prediction performance of related methods over the last 3-4 years. A particular reason is to make use of most advanced graph neural network based techniques, namely variational graph autoencoders as a deep generative model of utmost accuracy, the practical implementation of which¹⁹ was presented only a few months ago (just like the relevant network data). Note that only this recent implementation enables to process networks of sizes in the range of common molecular interaction data. In essence, graph neural networks “learn” the structure of links in networks, and infer rules that underlie the interplay of links. Based on the knowledge gained, they enable to predict links and output the corresponding links together with probabilities for them to indeed be missing.

Simulation experiments, reflecting scenarios where links known to exist in our network were re-established by prediction upon their removal, pointed out that our pipeline does indeed predict missing links at utmost accuracy.

Encouraged by these simulations, we proceeded by performing the core experiments, and predicted links to be missing without prior removal of links in our encompassing network. These core experiments revealed 692 high confidence interactions relating to 92 drugs. In our experiments, we focused on predicting links between drugs and human proteins that in turn are known to interact with SARS-CoV-2 proteins (SARS-CoV-2 associated host proteins). We have decidedly put the focus not on drug - SARS-CoV-2-protein interactions, which would have reflected more direct therapy strategies against the virus. Instead, we have focused on predicting drugs that serve the purposes of host-directed therapy (HDT) options, because HDT strategies have proven to be more sustainable with respect to mutations by which the virus escapes a response to the therapy applied. Note that HDT strategies particularly cater to drug repurposing attempts, because repurposed drugs have already proven to lack severe side effects, because they are either already in use, or have successfully passed the preclinical trial stages.

We further systematically categorized the 92 repurposable drugs into 70 categories based on their domains of application and molecular mechanism. According to this, we identified and highlighted several drugs that target host proteins that the virus needs to enter (and subsequently hijack) human cells. One such example is Captopril, which directly inhibits the production of Angiotensin-Converting Enzyme-2 (ACE-2), in turn already known to be a crucial host factor for SARS-CoV-2. Further, we identified Primaquine, as an antimalaria drug used to prevent the Malaria and also Pneumocystis pneumonia (PCP) relapses, because it interacts with the TIM complex TIMM29 and ALG11. Moreover, we have highlighted drugs that act as DNA replication inhibitor (Niclosamide, Anisomycin), glucocorticoid receptor agonists (Medrysone), ATPase inhibitors (Digitoxigenin, Digoxin), topoisomerase inhibitors (Camptothecin, Irinotecan), and proteosomal inhibitors (MG-132). Note that some drugs are known to have rather severe side effects from their original use (Doxorubicin, Vinblastine), but the disrupting effects of their short-term usage in severe COVID-19 infections may mean sufficient compensation.

In summary, we have compiled a list of drugs, which when repurposed are of great potential in the fight against the COVID-19 pandemic, where therapy options are urgently needed. Our list of predicted drugs suggests both options that had been identified and thoroughly discussed before and new opportunities that had not been pointed out earlier. The latter class of drugs may offer valuable chances for pursuing new therapy strategies against COVID-19.

Materials and Methods

Dataset Preparation

We have utilized three categories of interaction datasets: human protein-protein interactome data, SARS-CoV-2-host protein interaction data, and drug-host interaction data.

SARS-CoV-2-host Interaction Data

We have taken SARS-CoV-2–host interaction information from two recent studies by Gordon et al and Dick et al^{15,16}. In¹⁵, 332 high confidence interactions between SARS-CoV-2 and human proteins are predicted using using affinity-purification mass spectrometry (AP-MS). In¹⁶, 261 high confidence interactions are identified using sequence-based PPI predictors (PIPE4 & SPRINT).

Drug-Host Interactome Data

The drug–target interaction information has been collected from five databases, viz., DrugBank database (v4.3)⁵⁷, ChEMBL⁵⁸ database, Therapeutic Target Database (TTD)⁵⁹, PharmGKB database, and IUPHAR/BPS Guide to PHARMACOLOGY⁶⁰. Total number of drugs and drug-host interactions used in this study are 1309 and 1788407, respectively.

The Human Protein–Protein Interactome

We have built a comprehensive list of human PPIs from two datasets: (1) CCSB human Interactome database consisting of 7,000 genes, and 13944 high-quality binary interactions^{61–63}, (2) The Human Protein Reference Database⁵⁶ which consists of 8920 proteins and 53184 PPIs.

The summary of all the datasets is provided in Table 2. CMAP database²² is used to annotate the drugs with their usage different disease areas.

Sampling Strategy and Feature Matrix Generation

We have utilized *Node2vec*¹⁷, an algorithmic framework for learning continuous feature representations for nodes in networks. It maps the nodes to a low-dimensional feature space that maximizes the likelihood of preserving network neighborhoods.

The principle of feature learning framework in a graph can be described as follows: Let $G = (V, E)$ be a given graph, where V represents a set of nodes, and E represents the set of edges. The feature representation of nodes ($|V|$) is given by a mapping function: $f : V \rightarrow \mathbb{R}^d$, where d specify the feature dimension. The f may also be represented as a node feature matrix of dimension of $|V| \times d$. For each node, $v \in V$, $NN_S(v) \subset V$ defines a network neighborhood of node v which is generated using a neighbourhood sampling strategy S . The sampling strategy can be described as an interpolation between breadth-first search and depth-first search technique¹⁷. The objective function can be described as:

$$\max_f \left(\sum_{v \in V} \log P(NN_S(v) | f(v)) \right), \quad (1)$$

This maximizes the likelihood of observing a network neighborhood $NN_S(v)$ for a node v given on its feature representation f . Now the probability of observing a neighborhood node $n_i \in NN_S(v)$ given the feature representation of the source node v is given as :

$$P(NN_S(v) | f(v)) = \prod_{n_i \in NN_S(v)} P(n_i | f(v)). \quad (2)$$

where, n_i is the i^{th} neighbor of node v in neighborhood set $NN_S(v)$. The conditional likelihood of each source (v) and neighborhood node ($n_i \in NN_S(V)$) pair is represented as softmax of dot product of their features $f(v)$ and $f(n_i)$ as follows:

$$P(n_i | f(v)) = \frac{\exp(f(v) \cdot f(n_i))}{\sum_{u \in V} \exp(f(u) \cdot f(v))} \quad (3)$$

Variational Graph Auto Encoder

Variational Graph Autoencoder (VGAE) is a framework for unsupervised learning on graph-structured data⁶⁴. This model uses latent variables and is effective in learning interpretable latent representations for undirected graphs. The graph autoencoder consists of two stacked models: 1) Encoder and 2) Decoder. First, an encoder based on graph convolution networks (GCN)¹⁸ maps the nodes into a low-dimensional embedding space. Subsequently, a decoder attempts to reconstruct the original graph structure from the encoder representations. Both models are jointly trained to optimize the quality of the reconstruction from the embedding space, in an unsupervised way. The functions of these two model can be described as follows:

Encoder: It uses Graph Convolution Network (GCN) on adjacency matrix A and the feature representation matrix F . Encoder generates a d' -dimensional latent variable z_i for each node $i \in V$, with $|V| = n$, that corresponds to each embedding node, with $d' \leq n$. The inference model of the encoder is given below:

$$r(Z|A, F) = \prod_{i=1}^{|V|} r(z_i|A, F), \quad (4)$$

where, $r(z_i|A, F)$ corresponds to normal distribution, $\mathcal{N}(\frac{z_i}{\mu_i}, \sigma_i^2)$, μ_i and σ_i are the Gaussian mean and variance parameters. The actual embedding vectors z_i are samples drawn from these distributions.

Decoder: It is a generative model that decodes the latent variables z_i to reconstruct the matrix A using inner products with sigmoid activation from embedding vector, (Z).

$$\hat{A}_{i,j} = p(A_{i,j} = 1 | z_i, z_j) = \text{Sigmoid}(z_i^T \cdot z_j), \quad (5)$$

where, \hat{A} is the decoded adjacency matrix. The objective function of the variational graph autoencoder (VGAE) can be written as:

$$C_{VGAE} = E_{r(Z|A, F)} [\log p(A|Z)] - D_{KL}(r(Z|A, F) || p(Z)) \quad (6)$$

The objective function C_{VGAE} maximizes the likelihood of decoding the adjacency matrix w.r.t graph autoencoder weights using stochastic gradient decent. Here, $D_{KL}(\cdot || \cdot)$ represents Kullback-Leibler divergence⁶⁵ and $p(Z)$ is the prior distribution of latent variable.

Drug-SARS-CoV-2 Link Prediction

1. **Adjacency Matrix Preparation** In this work, we consider an undirected graph $G = (V, E)$ with $|V| = n$ nodes and $|E| = m$ edges. We denote A as the binary adjacency matrix of G . Here V consists of SARS-Cov-2 proteins, CoV-host proteins, drug-target proteins and drugs. The matrix (A) contains a total of $n = 16444$ nodes given as:

$$n = |N_{Nc}| + |N_{DT}| + |N_{NT}| + |N_D|, \quad (7)$$

where, N_{Nc} is the number of SARS-CoV-2 proteins. N_{DT} is the number of drug targets, whereas N_{NT} and N_D represent the number of CoV-host and drugs nodes, respectively. Total number of edges is given by:

$$m = |E_1| + |E_2| + |E_3|, \quad (8)$$

where, E_1 represents interactions between SARS-CoV-2 and human host proteins, E_2 is the number of interactions among human proteins, and E_3 represents the number of interactions between drugs and human host proteins.

2. **Feature Matrix Preparation:** The neighborhood sampling strategy is used here to prepare a feature representation of all nodes. A flexible biased random walk procedure is employed to explore the neighborhood of each node. A random walk in a graph G can be described as the probability:

$$P(a_i = x | a_{i-1} = v) = \pi(v, x), \quad (9)$$

where, $\pi(v, x)$ is the transition probability between nodes v and x , where $(v, x) \in E$ and a_i is the i^{th} node in the walk of length l . The transition probability is given by $\pi(v, x) = c_{pq}(t, x) * w_{vx}$, where t is the previous node of v in the walk, w_{vx} is the static edge weights and p, q are the two parameters which guides the walk. The coefficient $c_{pq}(t, x)$ is given by

$$c_{pq}(t, x) = \begin{cases} 1/p & \text{distance}(t, x) = 0 \\ 1 & \text{distance}(t, x) = 1 \\ 1/q & \text{distance}(t, x) = 2 \end{cases} \quad (10)$$

where, $distance(t, x)$ represents the shortest path distance between nodes t and node x . The process of feature matrix $F_{n \times d}$ generation is governed by the Node2vec algorithm. It starts from every nodes and simulates r random walks of fixed length l . In every step of walk transition probability $\pi(v, x)$ govern the sampling. The generated walk of each iteration is included to a walk-list. Finally, the stochastic gradient descent is applied to optimize the list of walks and result is returned.

3. **Link Prediction:** Scalable and Fast variational graph autoencoder (FastVGAE)¹⁹ is utilized in our proposed work to reduce the computational time of VGAE in large network. The adjacency matrix A and the feature matrix F are given into the encoder of FastVGAE. The encoder uses graph convolution neural network (GCN) on the entire graph to create the latent representation (Z).

$$Z = GCN(A, F) \quad (11)$$

The encoder works on full Adjacency Matrix A . After encoding, sampling is done and decoder works on the sampled sub graph.

The mechanism of decoder of FastVGAE is slightly different from traditional VGAE. It regenerate the adjacency matrix \hat{A} based on a subsample of graph nodes, V_s . It uses a graph node sampling technique to randomly sample the reconstructed nodes at each iteration. Each node is assigned with a probability p_i and the selection of nodes is based on the high score of p_i . The probability p_i is given by the following equation:

$$p(i) = \frac{f(i)^\alpha}{\sum_{j \in V} f(j)^\alpha}, \quad (12)$$

where, $f(i)$ is the degree of node i , and α is the sharpening parameter. We take $\alpha = 2$ in our study. The node selection process is repeated until $|V_s| = n_s$, where n_s is the number of sampling nodes.

The decoder reconstructs the smaller matrix, \hat{A}_s of dimension $n_s \times n_s$ instead of decoding the main adjacency matrix A . The decoder function follows the following equation:

$$\hat{A}_s(i, j) = Sigmoid(z_i^T \cdot z_j), \quad \forall (i, j) \in V_s \times V_s. \quad (13)$$

At each training iteration different subgraph (G_s) is drawn using the sampling method.

After the model is trained the drug–CoV-host links are predicted using the following equation:

$$p(A_{ij} = 1|z_i, z_j) = \text{Sigmoid}(z_i^T, z_j), \quad (14)$$

where A_{ij} represents the possible links between all combination of SARS-CoV-2 nodes and drug nodes. For each combination of nodes the model gives probability based on the logistic sigmoid function.

References

1. Wu, F. *et al.* A new coronavirus associated with human respiratory disease in china. *Nature* **579**, 265–269 (2020).
2. Forst, C. V. Host–pathogen systems biology. In *Infectious Disease Informatics*, 123–147 (Springer, 2010).
3. Kaufmann, S. H., Dorhoi, A., Hotchkiss, R. S. & Bartenschlager, R. Host-directed therapies for bacterial and viral infections. *Nat. Rev. Drug Discov.* **17**, 35 (2018).
4. Alaimo, S. & Pulvirenti, A. Network-based drug repositioning: Approaches, resources, and research directions. In *Computational Methods for Drug Repurposing*, 97–113 (Springer, 2019).
5. de Chasseay, B., Meyniel-Schicklin, L., Aublin-Gex, A., André, P. & Lotteau, V. New horizons for antiviral drug discovery from virus–host protein interaction networks. *Curr. opinion virology* **2**, 606–613 (2012).
6. Emig, D. *et al.* Drug target prediction and repositioning using an integrated network-based approach. *PLoS One* **8** (2013).
7. Doolittle, J. M. & Gomez, S. M. Mapping protein interactions between dengue virus and its human and insect hosts. *PLoS neglected tropical diseases* **5** (2011).
8. Bandyopadhyay, S., Ray, S., Mukhopadhyay, A. & Maulik, U. A review of in silico approaches for analysis and prediction of hiv-1-human protein–protein interactions. *Brief. Bioinforma.* **16**, 830–851 (2015).
9. Mukhopadhyay, A. & Maulik, U. Network-based study reveals potential infection pathways of hepatitis-c leading to various diseases. *PloS one* **9** (2014).
10. Cao, H. *et al.* Prediction of the ebola virus infection related human genes using protein-protein interaction network. *Comb. chemistry & high throughput screening* **20**, 638–646 (2017).
11. Cheng, F. *et al.* A genome-wide positioning systems network algorithm for in silico drug repurposing. *Nat. communications* **10**, 1–14 (2019).
12. Zeng, X. *et al.* deepdr: a network-based deep learning approach to in silico drug repositioning. *Bioinformatics* **35**, 5191–5198 (2019).
13. Zhou, Y. *et al.* Network-based drug repurposing for novel coronavirus 2019-ncov/sars-cov-2. *Cell discovery* **6**, 1–18 (2020).
14. Li, X. *et al.* Network bioinformatics analysis provides insight into drug repurposing for covid-2019. *Preprints* (2020).
15. Gordon, D. E. *et al.* A sars-cov-2 protein interaction map reveals targets for drug repurposing. *Nature* 1–13 (2020).
16. Dick, K., Biggar, K. K. G. & R., J. Comprehensive prediction of the sars-cov-2 vs. human interactome using pipe4, sprint, and pipe-sites, DOI: [10.5683/SP2/JZ77XA](https://doi.org/10.5683/SP2/JZ77XA) (2020).
17. Grover, A. & Leskovec, J. node2vec: Scalable feature learning for networks. In *Proceedings of the 22nd ACM SIGKDD international conference on Knowledge discovery and data mining*, 855–864 (2016).
18. Kipf, T. N. & Welling, M. Variational graph auto-encoders. *arXiv preprint arXiv:1611.07308* (2016).
19. Salha, G., Hennequin, R., Remy, J.-B., Moussallam, M. & Vazirgiannis, M. Fastgae: Fast, scalable and effective graph autoencoders with stochastic subgraph decoding. *arXiv preprint* (2020).
20. Rossi, R. A. *et al.* From community to role-based graph embeddings. *arXiv preprint arXiv:1908.08572* (2019).
21. Wen, C.-C. *et al.* Specific plant terpenoids and lignoids possess potent antiviral activities against severe acute respiratory syndrome coronavirus. *J. medicinal chemistry* **50**, 4087–4095 (2007).
22. Subramanian, A. *et al.* A next generation connectivity map: L1000 platform and the first 1,000,000 profiles. *Cell* **171**, 1437–1452 (2017).
23. Beckett, S. J. Improved community detection in weighted bipartite networks. *Royal Soc. open science* **3**, 140536 (2016).

24. Wishart, D. S. *et al.* Drugbank: a comprehensive resource for in silico drug discovery and exploration. *Nucleic acids research* **34**, D668–D672 (2006).
25. Nepusz, T., Yu, H. & Paccanaro, A. Detecting overlapping protein complexes in protein-protein interaction networks. *Nat. methods* **9**, 471 (2012).
26. Salehi, B. *et al.* The therapeutic potential of apigenin. *Int. journal molecular sciences* **20**, 1305 (2019).
27. Zheng, B.-J. *et al.* Delayed antiviral plus immunomodulator treatment still reduces mortality in mice infected by high inoculum of influenza a/h5n1 virus. *Proc. Natl. Acad. Sci.* **105**, 8091–8096 (2008).
28. Leggio, L. *et al.* Baclofen promotes alcohol abstinence in alcohol dependent cirrhotic patients with hepatitis c virus (hcv) infection. *Addict. behaviors* **37**, 561–564 (2012).
29. Jasso-Miranda, C. *et al.* Antiviral and immunomodulatory effects of polyphenols on macrophages infected with dengue virus serotypes 2 and 3 enhanced or not with antibodies. *Infect. drug resistance* **12**, 1833 (2019).
30. Maschera, B., Ferrazzi, E., Rassa, M., Toni, M. & Palu, G. Evaluation of topoisomerase inhibitors as potential antiviral agents. *Antivir. Chem. Chemother.* **4**, 85–91 (1993).
31. Gonzalez-Molleda, Y. Y., Lorenzo Wang & Yan. Potent antiviral activity of topoisomerase i and ii inhibitors against kaposi's sarcoma-associated herpesvirus. *Antimicrob. agents chemotherapy* **56**, 893–902 (2012).
32. Horwitz, S. B., Chang, C.-K. & Grollman, A. P. Antiviral action of camptothecin. *Antimicrob. agents chemotherapy* **2**, 395–401 (1972).
33. Bennett, R. P. *et al.* An analog of camptothecin inactive against topoisomerase i is broadly neutralizing of hiv-1 through inhibition of vif-dependent apobec3g degradation. *Antivir. research* **136**, 51–59 (2016).
34. Pantazis, P., Han, Z., Chatterjee, D. & Wyche, J. Water-insoluble camptothecin analogues as potential antiviral drugs. *J. biomedical science* **6**, 1–7 (1999).
35. Fillion, L., Logan, D., Gaudreault, R. & Izaguirre, C. Inhibition of hiv-1 replication by daunorubicin. *Clin. investigative medicine. Med. clinique et experimentale* **16**, 339–347 (1993).
36. Kaptein, S. J. *et al.* A derivate of the antibiotic doxorubicin is a selective inhibitor of dengue and yellow fever virus replication in vitro. *Antimicrob. agents chemotherapy* **54**, 5269–5280 (2010).
37. Johansson, S., Goldenberg, D. M., Griffiths, G. L., Wahren, B. & Hinkula, J. Elimination of hiv-1 infection by treatment with a doxorubicin-conjugated anti-envelope antibody. *Aids* **20**, 1911–1915 (2006).
38. Huang, Q. *et al.* Antiviral activity of mitoxantrone dihydrochloride against human herpes simplex virus mediated by suppression of the viral immediate early genes. *BMC microbiology* **19**, 274 (2019).
39. Matalon, S., Rasmussen, T. A. & Dinarello, C. A. Histone deacetylase inhibitors for purging hiv-1 from the latent reservoir. *Mol. medicine* **17**, 466–472 (2011).
40. Archin, N. M. *et al.* Interval dosing with the hdac inhibitor vorinostat effectively reverses hiv latency. *The J. clinical investigation* **127**, 3126–3135 (2017).
41. Lauer, S. A. *et al.* The incubation period of coronavirus disease 2019 (covid-19) from publicly reported confirmed cases: estimation and application. *Annals internal medicine* (2020).
42. Ju, H.-Q. *et al.* Synthesis and in vitro anti-hsv-1 activity of a novel hsp90 inhibitor bj-b11. *Bioorganic medicinal chemistry letters* **21**, 1675–1677 (2011).
43. Shim, H. Y., Quan, X., Yi, Y.-S. & Jung, G. Heat shock protein 90 facilitates formation of the hbv capsid via interacting with the hbv core protein dimers. *Virology* **410**, 161–169 (2011).
44. DeDiego, M. L. *et al.* Severe acute respiratory syndrome coronavirus envelope protein regulates cell stress response and apoptosis. *PLoS pathogens* **7** (2011).
45. Wang, Y. *et al.* Hsp90: a promising broad-spectrum antiviral drug target. *Arch. virology* **162**, 3269–3282 (2017).
46. Sultan, I., Howard, S. & Tbakhi, A. Drug repositioning suggests a role for the heat shock protein 90 inhibitor geldanamycin in treating covid-19 infection. *arXiv* (2020).
47. Xu, J., Shi, P.-Y., Li, H. & Zhou, J. Broad spectrum antiviral agent niclosamide and its therapeutic potential. *ACS infectious diseases* (2020).
48. Liu, J. *et al.* Hydroxychloroquine, a less toxic derivative of chloroquine, is effective in inhibiting sars-cov-2 infection in vitro. *Cell discovery* **6**, 1–4 (2020).

49. Vöhringer, H.-F. & Arastéh, K. Pharmacokinetic optimisation in the treatment of pneumocystis carinii pneumonia. *Clin. pharmacokinetics* **24**, 388–412 (1993).
50. Amarelle, L. & Lecuona, E. The antiviral effects of na, k-atpase inhibition: A minireview. *Int. journal molecular sciences* **19**, 2154 (2018).
51. Schneider, M. *et al.* Severe acute respiratory syndrome coronavirus replication is severely impaired by mg132 due to proteasome-independent inhibition of m-calpain. *J. virology* **86**, 10112–10122 (2012).
52. Lin, S.-C. *et al.* Effective inhibition of mers-cov infection by resveratrol. *BMC infectious diseases* **17**, 144 (2017).
53. Shang, J. *et al.* Structural basis of receptor recognition by sars-cov-2. *Nature* 1–4 (2020).
54. Gurwitz, D. Angiotensin receptor blockers as tentative sars-cov-2 therapeutics. *Drug development research* (2020).
55. Yu, H. *et al.* Next-generation sequencing to generate interactome datasets. *Nat. methods* **8**, 478 (2011).
56. Peri, S. *et al.* Development of human protein reference database as an initial platform for approaching systems biology in humans. *Genome research* **13**, 2363–2371 (2003).
57. Law, V. *et al.* Drugbank 4.0: shedding new light on drug metabolism. *Nucleic acids research* **42**, D1091–D1097 (2014).
58. Gaulton, A. *et al.* ChEMBL: a large-scale bioactivity database for drug discovery. *Nucleic acids research* **40**, D1100–D1107 (2012).
59. Yang, H. *et al.* Therapeutic target database update 2016: enriched resource for bench to clinical drug target and targeted pathway information. *Nucleic acids research* **44**, D1069–D1074 (2016).
60. Pawson, A. J. *et al.* The iuphar/bps guide to pharmacology: an expert-driven knowledgebase of drug targets and their ligands. *Nucleic acids research* **42**, D1098–D1106 (2014).
61. Rual, J.-F. *et al.* Towards a proteome-scale map of the human protein–protein interaction network. *Nature* **437**, 1173–1178 (2005).
62. Rolland, T. *et al.* A proteome-scale map of the human interactome network. *Cell* **159**, 1212–1226 (2014).
63. Luck, K. *et al.* A reference map of the human binary protein interactome. *Nature* **580**, 402–408 (2020).
64. Rezende, D. J., Mohamed, S. & Wierstra, D. Stochastic backpropagation and approximate inference in deep generative models. *arXiv preprint arXiv:1401.4082* (2014).
65. Kullback, S. & Leibler, R. A. On information and sufficiency. *The annals mathematical statistics* **22**, 79–86 (1951).

Acknowledgements

S.Ray acknowledges support from ERCIM Alain Bensoussan Fellowship programme grant. S.Bandyopadhyay acknowledges support from J.C. Bose Fellowship [SB/S1/JCB-033/2016 to S.B.] by the DST, Govt. of India; SyMeC Project grant [BT/Med-II/NIBMG/SyMeC/2014/Vol. II] was given to the Indian Statistical Institute by the Department of Biotechnology (DBT), Govt. of India. A. Mukhopadhyay acknowledges the support received from the research project grant (Memo No: 355(Sanc.)/ST/P/S&T/6G-10/2018 dt. 08/03/2019) of Dept. of Science & Technology and Biotechnology, Govt. of West Bengal, India.

Availability: All codes and datasets are given in the github link:
<https://github.com/sumantaray/Covid19>